THE JOURNAL OF BIOLOGICAL CHEMISTRY VOL. 288, NO. 35, pp. 25119–25128, August 30, 2013

Dual Role of BAR Domain-containing Proteins in Regulating Vesicle Release Catalyzed by the GTPase, Dynamin-2*[S]

Received for publication, June 3, 2013, and in revised form, June 30, 2013 Published, JBC Papers in Press, July 16, 2013, DOI 10.1074/jbc.M113.490474

Sylvia Neumann and Sandra L. Schmid[1]

From the Department of Cell Biology, The Scripps Research Institute, La Jolla, California 92037

Background: Membrane curvature generation is essential for dynamin-2-catalyzed membrane fission and vesicle release.
Results: Dynamin-2 binding partners with curvature generating activity differentially regulate the assembly, GTPase, and fission activities of dynamin-2.
Conclusion: Dynamin-2 partners display complex patterns of regulation.
Significance: The distinct functional interactions between dynamin-2 and its binding partners position them to contribute to the spatio-temporal regulation of clathrin-mediated endocytosis.

Dynamin-2 (Dyn2) is ubiquitously expressed and catalyzes membrane fission during clathrin-mediated endocytosis in nonneuronal cells. We have previously shown that Dyn2 inefficiently generates membrane curvature and only mediates fission of highly curved membranes. This led to the hypothesis that other endocytic accessory proteins (EAPs) generate curvature needed to sculpt a sufficiently narrow neck to trigger Dyn2 assembly and fission. Candidates for this activity are EAPs that bind to the dynamin proline/arginine-rich domain (PRD) through their SH3 (src homology-3) domains and also encode curvature-generating BAR (Bin/Amphiphysin/Rvs) domains. We show that at low concentrations, amphiphysin and endophilin, but not SNX9 or the curvature-generating epsin N-terminal homology (ENTH) domain, are able to generate tubules from planar membrane templates and to synergize with Dyn2ΔPRD to catalyze vesicle release. Unexpectedly, SH3-PRD interactions were inhibitory and reciprocally regulate scaffold assembly. Of the three proteins studied, only full-length amphiphysin functions synergistically with full-length Dyn2 to catalyze vesicle release. The differential activity of these proteins correlates with the relative potency of their positive, curvature-generating activity, and the negative regulatory effects mediated by SH3 domain interactions. Our findings reveal opportunities for the spatio-temporal coordination of membrane curvature generation, dynamin assembly, and fission during clathrin-mediated endocytosis.

Clathrin-mediated endocytosis (CME)[2] is a highly regulated process orchestrated by a complex protein machinery. It occurs via clathrin-coated pits (CCPs), whose formation is initiated by adaptor proteins that capture cargo molecules and trigger clathrin assembly at the plasma membrane. Subsequent recruitment of endocytic accessory proteins (EAPs) drives the maturation of a deeply invaginated coated pit (1, 2). The large GTPase dynamin is recruited to nascent CCPs and regulates CCP maturation (3, 4). At later stages, dynamin self-assembles into collar-like structures at the constricted neck of a pit and catalyzes membrane fission leading to clathrin-coated vesicle (CCV) release (5, 6).

Dynamin-catalyzed membrane fission can be directly measured *in vitro* using SUPER templates (supported bilayers with excess membrane reservoir) as a membrane substrate (7, 8) and by following the release of fluorescently labeled lipid vesicles either by light microscopy or by a simple sedimentation assay. Using these assays, we demonstrated that dynamin-1 (Dyn1), the neuron-specific isoform, alone was sufficient to generate membrane curvature (*i.e.* tubulation) in the absence of GTP and to release vesicles from SUPER templates in a GTPase-dependent manner (7). Although dynamin-2 (Dyn2), the ubiquitously-expressed isoform, can assemble onto curved templates and catalyze fission, it is much less efficient than Dyn1 in generating membrane curvature and thus catalyzing vesicle release from planar membranes (9). These results suggest that other curvature-generating EAPs function upstream to generate the narrow neck needed to activate Dyn2 for CCV release.

Among EAPs, Bin/Amphiphysin/Rvs (BAR) domain-containing proteins and epsin N-terminal homology (ENTH) domain-containing proteins have been identified as curvature generators that can mediate deformation of liposomes *in vitro* and induce membrane tubulation when overexpressed *in vivo* (10–15). Structural analyses showed that BAR domains form crescent shaped dimers that bind and assemble into scaffolds that can impose their intrinsic curvature onto the underlying membrane (12, 14, 16–18). In addition, the N-BAR domains of amphiphysin and endophilin contain an N-terminal amphipathic helix that inserts into the membrane and facilitates membrane binding, curvature sensing, and generation (12, 14, 18–20). In contrast, ENTH domains do not possess intrinsic curvature but contain an N-terminal amphipathic helix that inserts into the bilayer resulting in membrane deformation and tubulation at high concentrations (21, 22). How-

* This work was supported, in whole or in part, by National Institutes of Health Grants R01GM42455 and MH61345 (to S. L. S.) and an AHA Fellowship (to S. N.).
[S] This article contains supplemental movies S1–S6.
[1] To whom correspondence should be addressed: Department of Cell Biology, UT Southwestern Medical Center 5323 Harry Hines Boulevard, Dallas, TX 75390. E-mail: sandra.schmid@utsouthwestern.edu.
[2] The abbreviations used are: CME, clathrin-mediated endocytosis; CCP, clathrin-coated pit; EAP, endocytic accessory protein; PRD, proline/arginine-rich domain; BAR, Bin/Amphiphysin/Rvs; ENTH, epsin N-terminal homology; CCV, clathrin-coated vesicle; Dyn, dynamin; Lqf, Liquid facets.

ever, it has been recently suggested that epsin also forms higher order assemblies when bound to membranes, which might contribute to curvature generation (23, 24).

Several BAR domain-containing proteins, including endophilin, amphiphysin, and SNX9 also encode SH3 domains and interact directly with dynamin through its C-terminal proline/arginine-rich domain (PRD). *In vitro* studies have shown that these proteins can also regulate dynamin self-assembly, membrane binding, and GTPase activity (25–31). Thus, these proteins are good candidates for EAPs that could function, together with Dyn2, to enhance fission. However, recent studies have suggested that BAR domain protein scaffolds antagonize membrane fission by stabilizing curved membranes (32), whereas hydrophobic insertions by ENTH domains, in the absence of scaffolding activity, create sufficient membrane defects to facilitate the reorganization of lipids required to enable membrane fission. Indeed, this report showed that, when expressed at high concentrations, epsin can support CME in cells depleted of dynamin by siRNA.

Here, we have systematically studied the effects of BAR domain-containing dynamin binding partners, amphiphysin, endophilin, and SNX9, as well as epsin, on dynamin-catalyzed vesicle release from planar SUPER templates. Our results reveal complexity in the functional interplay between dynamin and its SH3 and BAR-domain containing partners that may reflect a hierarchy of interactions that combine to regulate curvature generation and dynamin activity in CME.

EXPERIMENTAL PROCEDURES

Protein Purification—Dyn1, Dyn2, and various mutants were expressed from pIEX-6. Constructs were transiently transfected in Sf9 cells as previously described (33) and purified by affinity chromatography as described previously using glutathione *S*-transferase (GST)-tagged amphiphysin-II SH3 domain as an affinity ligand (34). Purified dynamin was dialyzed overnight in 20 mM HEPES pH 7.5, 150 mM KCl, 1 mM DTT, 1 mM EGTA, and 10% glycerol and stored at −80 °C. The endophilin N-BAR domain and mutant was a kind gift from Naoki Muchizuki (RIKEN Harima Institute, Japan, (14)). Full-length effector proteins (amphiphysin I, endophilin I, and SNX9) and endophilin N-BAR domain and Epsin 1 ENTH domain were expressed from pGEX6P. The SH3-domain from amphiphysin, endophilin, and SNX9 as well as the PRD of Dyn1 and Dyn2 were expressed from pGEX2T. Constructs were transformed into BL21. Protein expression was induced with 1 mM IPTG at OD_{600} ~0.7 for 3 h at 30 °C. Proteins were purified following the manufacturer's instructions, and the GST tag was removed with Prescission Protease (GE Life Sciences, Piscataway, NJ) from constructs expressed from pGEX6P. Proteins were stored in 50 mM Tris, 200 mM NaCl, and 1 mM DTT and 10% glycerol at −80 °C.

Preparation of Lipid Templates—For liposomes, lipid mixtures (DOPC:DOPS:PIP2 80:15:5) were dried and rehydrated in buffer (20 mM HEPES, pH 7.5, and 150 mM KCl) to a final concentration of 1 mM, and subjected to a series of freeze-thaw cycles before extrusion through polycarbonate membranes (Whatman, Clifton, NJ) with a pore size of 1 μm using an Avanti Mini-Extruder. SUPER templates were generated as previously reported (7, 35), all solutions for their preparation were filtered through a 0.22-μm filter, and incubations were performed in low adhesion microcentrifuge tubes (USA Scientific). Briefly, silica beads (5×10^6 silicon oxide microspheres d = 4.97 μm, or 15×10^6 silicon oxide microspheres d = 2.5 μm Corpuscular, Cold Spring, NY) were incubated with 20 nmol of 100 nm extruded liposomes (DOPC:DOPS:PIP2:RhoPE 79:15:5:1) in 20 mM HEPES pH 7.5 and 1 M NaCl for 5 μm silica beads or 200 mM NaCl for 2.5 μm silica beads in a final volume of 100 μl. The mix was incubated for 30 min at room temperature. To wash the templates 1 ml of water was added, and tubes were centrifuged in a swing-out centrifuge rotor (Allegra™ 6R Centrifuge, Beckman). 1 ml of supernatant was removed by pipetting, and the residual 100 μl reaction was mixed with 1 ml of water by gentle vortexing (medium speed), and washing was repeated four times.

Vesicle Release from SUPER Templates—All experiments were performed in low adhesion microcentrifuge tubes (USA Scientific). To measure vesicle release 5×10^5 of 5 μm templates or 20×10^5 of 2.5 μm templates were added to buffer containing 20 mM HEPES pH 7.5, 150 mM KCl, 1 mM $MgCl_2$, 1 mM GTP at a final volume of 100 μl and indicated concentrations of dynamin and effector proteins for 30 min at room temperature. During this incubation, templates were allowed to settle without further mixing. Templates were pelleted at 260 × *g* in a swing-out centrifuge rotor (Allegra™ 6R Centrifuge, Beckman), and 75 μl of the supernatants were mixed with 25 μl of 0.4% Triton X-100 to dissolve vesicles. Total fluorescence of templates was determined in a separate reaction containing the same amount of SUPER templates in 0.1% Triton X-100 in 20 mM HEPES pH 7.5, 150 mM KCl, 1 mM $MgCl_2$. Fluorescence was measured in a 96 well fluorescent plate reader (Bio-Tek Instruments) and vesicle release is expressed as RhPE released into the supernatant as percentage of total RhPE fluorescence of SUPER templates (35). Fluorescence released in the absence of GTP is subtracted as background.

Fluorescent Microscopy of Protein-SUPER Template Interactions—Assays for fission activity on membrane tethers were performed in Lab-Tek chambers (Nunc) that had been preincubated for 20 min with 2 mg/ml BSA. These were washed and 200 μl of 20 mM HEPES pH 7.5, 150 mM KCl, 1 mM $MgCl_2$, 1 mM GTP with an oxygen scavenger system, which was essential to prevent photo-damage of proteins, that consisted of 50 μg/ml glucose oxidase (Sigma), 10 μg/ml catalase (Roche), 2.5 mM glucose (Sigma), and 1 mM DTT was added. To this, we added 5×10^5 SUPER templates and allowed them to settle onto the coverslip. Tethers were generated by the addition of 20 μm naked silica beads, which were gently rolled over the surface of the SUPER templates through gentle agitation of the Lab-Tek chamber. Fluorescence imaging was carried out at room temperature on an inverted Olympus IX-70 microscope with a 100×, 1.35 NA oil-immersion objective, and equipped with an ORCA ER CCD camera (Hamamatsu) and 617/73 nm emission filters for RhPE-labeled membranes. Dynamin or ENTH domain was added at the indicated concentration to the corner and allowed to diffuse across the chamber. Curvature generation experiments were executed as above except that SUPER templates were allowed to settle in a buffer containing

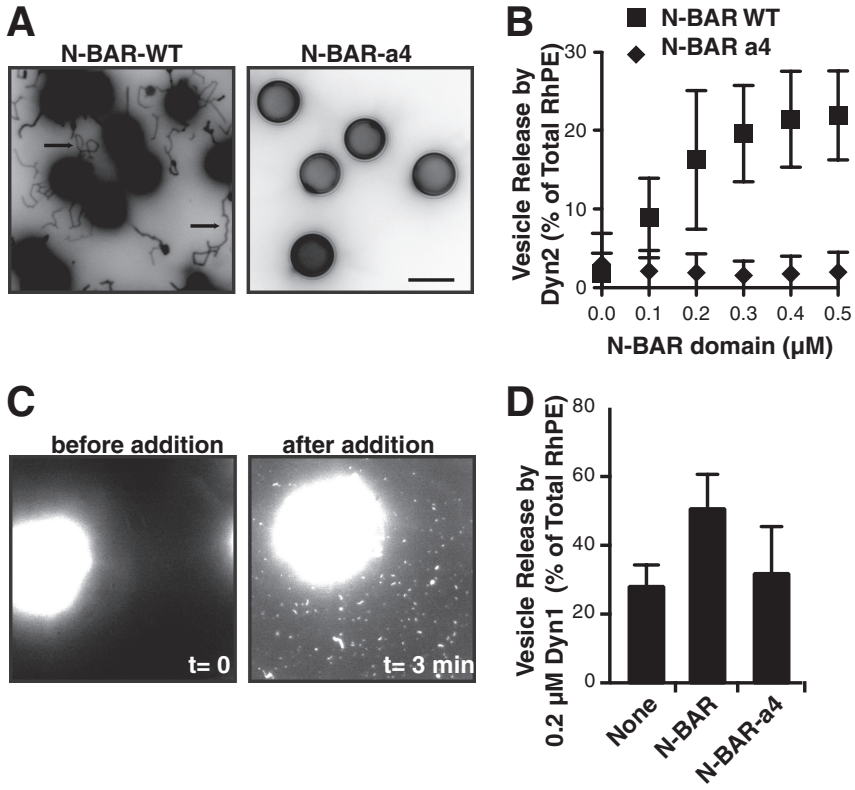

FIGURE 1. **Endophilin N-BAR stimulates Dyn2-catalyzed vesicle release.** *A*, tubulation of SUPER templates. SUPER templates were dispersed into assay buffer containing an oxygen scavenger system in the presence of 0.5 μM N-BAR WT or N-BAR a4 for 10 min at room temperature. Images are inverted in contrast for clarity, and *arrows* indicate tubules. *Scale bar* is 5 μm. *B*, Dyn2 (0.5 μM) was incubated with SUPER templates for 30 min at room temperature with increasing concentrations of either endophilin N-BAR WT or a mutant deficient in curvature generation, N-BAR a4. Vesicle release was measured by the appearance of fluorescent RhPE in the supernatant after sedimentation of the SUPER templates. Fluorescence released in the absence of GTP was subtracted as background (shown are averages ± S.D., $n = 9$). SUPER templates were dispersed into assay buffer containing an oxygen scavenger system and 1 mM GTP. After the templates had settled, imaging was started and Dyn2 and N-BAR domain were added together to the solution with a pipette to a final concentration of 0.5 μM. The micrograph shows a field of view before (*left panel*) and after (*right panel*) addition of Dyn2 and N-BAR. See supplemental Movie S1 for full sequence. *Scale bar* is 5 μm. *D*, Dyn1 (0.2 μM) was incubated with SUPER templates for 30 min at room temperature without or with 0.5 μM endophilin N-BAR or N-BAR-a4, as above (shown are averages ± S.D., $n > 3$).

0.5 μM dynamin or effector proteins without GTP. Pictures were taken after an incubation of 10 min at room temperature.

GTPase Activity—GTP hydrolysis by dynamin was measured as a function of time using a colorimetric malachite green assay that detects the release of inorganic phosphate (36). Briefly, 0.5 μM dynamin with or without 0.5 μM effector protein were added to 150 μM 1 μm liposomes in a buffer containing 20 mM HEPES pH 7.5, 150 mM KCl, 1 mM GTP, and 2 mM $MgCl_2$. Aliquots were taken at several time points. Free phosphate was determined using malachite green and rates of hydrolysis were calculated.

RESULTS

Curvature Generation by the Endophilin N-BAR Domain Facilitates Dyn2-catalyzed Vesicle Release—We previously showed that Dyn2 was less effective than Dyn1 at catalyzing vesicle release from SUPER templates because it was less effective at generating curvature on planar lipid templates (9). We therefore tested whether curvature-generating N-BAR domains might be able to function synergistically with Dyn2 to catalyze membrane fission. We first studied the well-characterized N-BAR domain of endophilin. Addition of 0.5 μM endophilin N-BAR domain to SUPER templates resulted in the formation of long membrane tubules. These concentrations are significantly lower than those used in most liposome tubulation assays (typically 5–10 μM), attesting to the efficient ability of endophilin N-BAR to generate curvature and self-assemble into a protein scaffold on these fluid membrane templates (Fig. 1*A*). In contrast, the N-BAR-a4 mutant, which bears a flexible insert that disrupts the rigid BAR domain dimer failed to tubulate SUPER templates. Masuda *et al.* (14) have shown that this mutant retains its ability to bind to liposomes, but is unable to generate curvature on these templates.

In the absence of dynamin, even at high concentrations, the wild-type endophilin N-BAR domain alone was unable to mediate fission of these tubules or to release vesicles from SUPER templates (results not shown). Likewise, when assayed at low concentrations, Dyn2-alone is inefficient at catalyzing vesicle release (Fig. 1*B* and Ref. 9). However, together the two functioned synergistically to efficiently release vesicles when incubated with SUPER templates (Fig. 1*B*). The ability of N-BAR to enhance Dyn2 activity plateaued at ~equimolar concentrations. N-BAR-a4 did not facilitate dynamin-catalyzed vesicle release, indicating that curvature generation by the N-BAR domain was essential for this activity. Vesicle release absolutely required the GTPase activity of Dyn2: the fluorescence released in the absence of GTP was equal to that released

in the absence of dynamin and was subtracted as background in all experiments. The endophilin N-BAR, but not N-BAR-a4, also functioned synergistically with subsaturating concentrations (0.2 μM) of Dyn1 (Fig. 1*D*). Again, the ability to support Dyn1 activity reached a plateau at ~equimolar N-BAR, without evidence of inhibition at higher concentrations of N-BAR (results not shown).

Vesicle release by Dyn1 can be visualized in real-time by fluorescence microscopy (7, 8). Although Dyn2 alone had very low activity in this assay, in the presence of wild type N-BAR domain we observed the release of both small vesicles and short tubules, which adsorbed onto the coverslip and were presumably coated with N-BAR and/or Dyn2 (supplemental movie S1). In summary, these experiments show that the curvature generating properties of the N-BAR domain work synergistically with Dyn2 to catalyze vesicle release.

Dynamin Requirements for Enhanced Vesicle Release in the Presence of the N-BAR Domain—We have previously shown that efficient vesicle release by Dyn1 requires both insertion of hydrophobic residues located within the variable loops 1 and 3 (VL1 and VL3) of its PH domain (9, 33), as well as its ability to self-assemble (7, 38) and to trigger coordinated GTP hydrolysis (39). Recent studies have shown that at high concentrations (2–4 μM) insertion of the amphipathic helices of epsin's ENTH domain or N-BAR domains into the lipid bilayer can also mediate vesicle fragmentation (32). Given this observation, we tested whether the presence of the endophilin N-BAR domain might relieve the requirement for insertion of Dyn1's hydrophobic VL1 loop to catalyze vesicle release. Indeed, the *in vitro* fission activity of the VL1/I533A mutant of Dyn1, which is defective in membrane curvature generation and vesicle release, could be completely complemented by addition of the N-BAR domain (Fig. 2*A*), providing strong evidence that the two proteins can work cooperatively to catalyze vesicle release. Importantly, overexpression of Dyn1(I533A) strongly inhibits clathrin-mediated endocytosis (33), indicating differences in the *in vivo* requirements for CCV release relative to those required for vesicle release from SUPER templates. These differences may relate to membrane tension, relative concentrations of the Dyn2 and N-BAR proteins, and/or, as described below, differences in activities of full-length *versus* truncated N-BAR proteins. Clearly, much more work is needed to fully reconstitute CCV formation *in vitro*.

Recent biochemical (39) and biophysical (40) evidence suggests that the minimal unit for efficient dynamin-catalyzed fission is a two-rung structure. Yet, it has also been suggested that the scaffolding activity of dynamin, might oppose fission mediated by the amphipathic helix insertions of ENTH (or N-BAR) domains (32). Thus, we wondered whether the minimal unit for dynamin-catalyzed fission might be different when functioning together with N-BAR domains. To test this we measured vesicle release from SUPER templates by a fixed concentration of WT Dyn1 in the presence of increasing concentrations of a GTPase-defective mutant, S45N, which will co-assemble with WT protein. We used Dyn1 for these experiments because it efficiently catalyzes membrane fission on its own. As we previously reported (39), the fission activity of Dyn1 was highly sensitive to inhibition by the S45N mutant (Fig. 2*B*), indicating that coordinated GTPase activity of subunits within an assembled dynamin collar is necessary for efficient fission activity. Under these subsaturating conditions, addition of the N-BAR domain stimulates Dyn1-mediated vesicle release (results not shown), therefore the data are normalized to directly compare the effects of S45N addition on Dyn1 fission activity in the presence or absence of the N-BAR domain. In the presence of the N-BAR domain, Dyn1-catalyzed vesicle release is, if anything, more sensitive to inhibition by S45N (Fig. 2*B*), indicating that the need for coordinated GTP hydrolysis between assembled dynamin rungs remains, regardless of the synergistic effects of N-BAR domains.

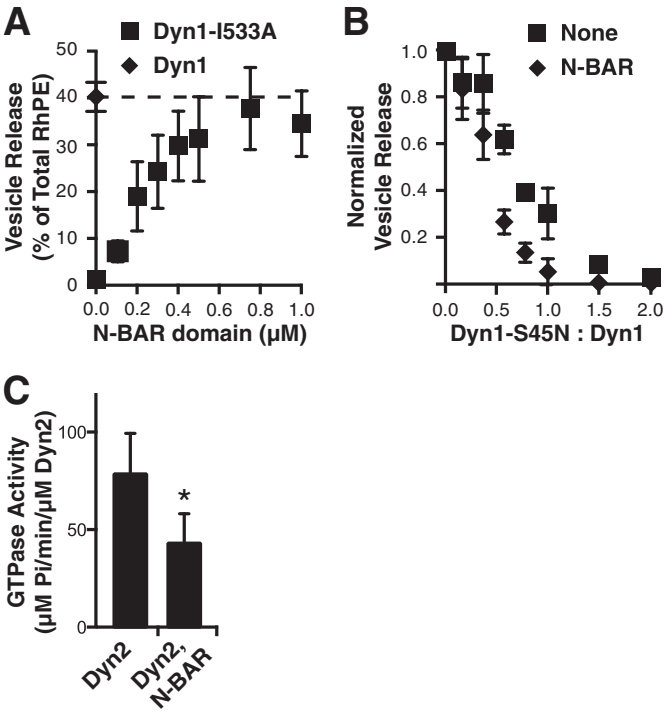

FIGURE 2. **Properties of synergistic N-BAR and dynamin-catalyzed vesicle release.** *A*, vesicle release catalyzed by 0.5 μM Dyn1-I533A mutant in the presence of increasing concentrations of the endophilin N-BAR domain (shown are averages ± S.D., $n > 4$). *B*, inhibition of vesicle release catalyzed by either 0.5 μM Dyn1 (*squares*) or 0.5 μM of both Dyn1 and the endophilin N-BAR domain (*diamonds*) by increasing concentrations of the dominant negative Dyn1-S45N mutant (shown are averages ± S.D., $n = 4$). Fluorescence released in the absence of GTP was subtracted as background. *C*, assembly-stimulated GTPase activity of Dyn2, or Dyn2+endophilin N-BAR measured on 1 μm liposomes at a final concentration of 0.5 μM (shown are averages ± S.D., $n = 4$, *, $p < 0.05$).

N-BAR Domain Inhibits Dyn2 Assembly-stimulated GTPase Activity—We next examined the effect on the N-BAR domain on the GTPase activity of Dyn2 using large (1 μm) liposomes as pseudo-planar lipid templates. Unexpectedly, Dyn2 assembly-stimulated GTPase activity was strongly inhibited in the presence of the N-BAR domain (Fig. 2*C*). Previous studies have shown that dynamin-catalyzed membrane fission is a stochastic process involving many, apparently futile cycles of assembly/disassembly driven by GTP hydrolysis (7, 40, 41). While we cannot directly measure the relationship between GTP hydrolysis and individual membrane fission events, these data suggest that the presence of the N-BAR domain increases the efficiency of coupling between dynamin GTPase activity and membrane fission.

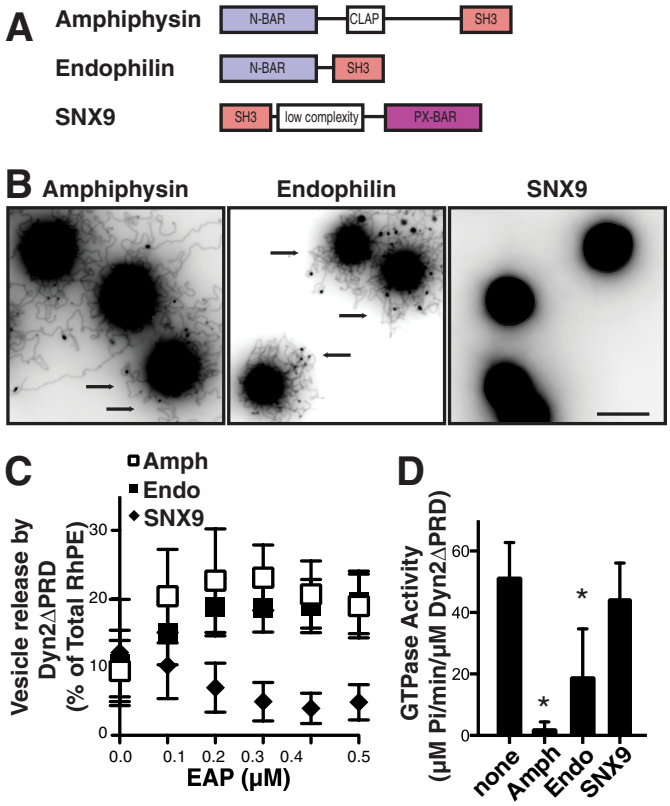

FIGURE 3. **Differential effects of BAR domain-containing proteins on Dyn2-ΔPRD-catalyzed vesicle release and assembly-stimulated GTPase activity.** *A*, domain structure of the dynamin binding partners amphiphysin, endophilin, and SNX9. All three proteins contain an SH3 domain for their interaction with dynamin. Amphiphysin and endophilin contain an N-BAR domain, characterized by its amphipathic helix involved in curvature generation, SNX9 contains a BAR domain adjacent to a phosphoinositide binding PX domain. CLAP is a clathrin, AP2 binding domain. *B*, tubulation of SUPER templates, by 0.5 μM amphiphysin, endophilin or SNX9 assayed as described in Fig. 1*A*. Images are inverted in contrast for clarity, and *arrows* indicate tubules. *Scale bar* is 5 μm. *C*, vesicle release from SUPER templates by Dyn2-ΔPRD (0.5 μM) alone or in the presence of increasing concentrations of amphiphysin, endophilin, or SNX9. Fluorescence released in the absence of GTP was subtracted as background (shown are averages ± S.D., n > 7). *D*, assembly-stimulated GTPase activity of Dyn2-ΔPRD, or Dyn2-ΔPRD in the presence of amphiphysin, endophilin, and SNX9 measured on 1 μm liposomes at a final concentration of 0.5 μM (shown are averages ± S.D., $n = 6$. *, $p < 0.001$).

Full-length Endophilin and Amphiphysin but Not SNX9 Stimulate Dyn2-catalyzed Vesicle Release—Next, we tested the ability of full-length dynamin binding partners amphiphysin, endophilin, and sorting nexin 9 (SNX9) (Fig. 3*A*), to stimulate Dyn2-catalyzed vesicle release. Unlike amphiphysin and endophilin, which encode N-BAR domains, SNX9 encodes a PX-BAR domain, known to be less efficient in curvature generation (42, 43). Consistent with these classifications, full-length amphiphysin and endophilin efficiently generated long membrane tubules from SUPER templates at submicromolar concentrations (Fig. 3*B*); whereas, SNX9 could not generate membrane tubules (Fig. 3*B*) even at a concentration of 1.0 μM (results not shown).

Through direct SH3-PRD interactions, these proteins can regulate dynamin self-assembly, GTPase activity and membrane binding (25–31). In order to uncouple the effect of curvature generation by their BAR domains from other effects on dynamin activity, we initially tested the ability of these proteins to synergize with truncated Dyn2 lacking its PRD (Dyn2ΔPRD). In a concentration-dependent manner, with maximal activity occurring at equimolar concentrations (Fig. 3*C*) both amphiphysin and endophilin enhanced Dyn2ΔPRD-catalyzed membrane fission, whereas SNX9 was slightly inhibitory. Their ability to enhance Dyn2ΔPRD-catalyzed fission paralleled their relative abilities to generate membrane curvature on SUPER templates (Fig. 3*B*). Similar to the effects of the endophilin N-BAR domain, amphiphysin, and endophilin inhibited the assembly stimulated GTPase activity of Dyn2ΔPRD, whereas SNX9 had no effect (Fig. 3*D*).

PRD-SH3 Interactions Inhibit Dyn2-catalyzed Vesicle Release—The above data show that the efficiency of Dyn2 (or, at limiting concentrations Dyn1)-catalyzed vesicle release is enhanced by the curvature generating effects of N-BAR domains on the planar lipid substrate. To determine whether the ability of these dynamin partners to regulate other aspects of dynamin function affects its membrane fission activity, we next tested the ability of full-length amphiphysin, endophilin, and SNX9 to synergize with full-length Dyn2 to catalyze vesicle release. Interestingly, the three dynamin binding partners affected full-length Dyn2 catalyzed vesicle release in three different ways: amphiphysin stimulated Dyn2-catalyzed vesicle release, endophilin had no significant effect, and SNX9 was inhibitory (Fig. 4*A*). As above, the effects of these binding partners on dynamin catalyzed vesicle release were inversely correlated with their effects on dynamin assembly-stimulated GTPase activity (Fig. 4*B*).

The differential effects of endophilin and SNX9 on full-length *versus* Dyn2ΔPRD, suggest that interactions between their SH3 domains and Dyn2 PRD inhibit the ability of Dyn2 to release vesicles. We tested this directly by measuring Dyn2-catalyzed vesicle release in the presence of increasing concentrations of purified GST-tagged SH3 domains from each of the BAR domain-containing binding partners. Because vesicle release by Dyn2 alone is relatively low, these experiments were performed using 1.0 μM Dyn2 (Fig. 4*C*) and also with 0.5 μM Dyn1, which on its own could effectively mediate vesicle release from SUPER templates (Fig. 4*D*). As predicted, increasing concentrations of endophilin and SNX9 SH3 domains potently inhibited Dyn2 (and Dyn1)-catalyzed vesicle release (50% inhibition at a ratio of 0.25 SH3 domains/dynamin). The amphiphysin SH3 domain was also inhibitory, but at ~4-fold higher concentrations (50% inhibition at a ratio of >1:1 SH3 domain:Dyn2).

Dynamin and Its Binding Partners Reciprocally Regulate Each Other's Membrane Tubulation Activities—To gain more insight as to how PRD-SH3 domain interactions inhibit the synergistic activity of Dyn2 and its N-BAR-containing partners, we performed tubulation assays, which measure the combined activities of proteins to bind to membranes, generate membrane curvature and, importantly, form long scaffolds on these planar membrane templates. As described above, both amphiphysin and endophilin are able to form tubules from SUPER templates (Fig. 5*A*). In contrast, when Dyn2 is added to the incubations in the absence of GTP to prevent fission, no tubules were detected. Even after amphiphysin has formed tubules, the addition of Dyn2 in the absence of GTP causes their

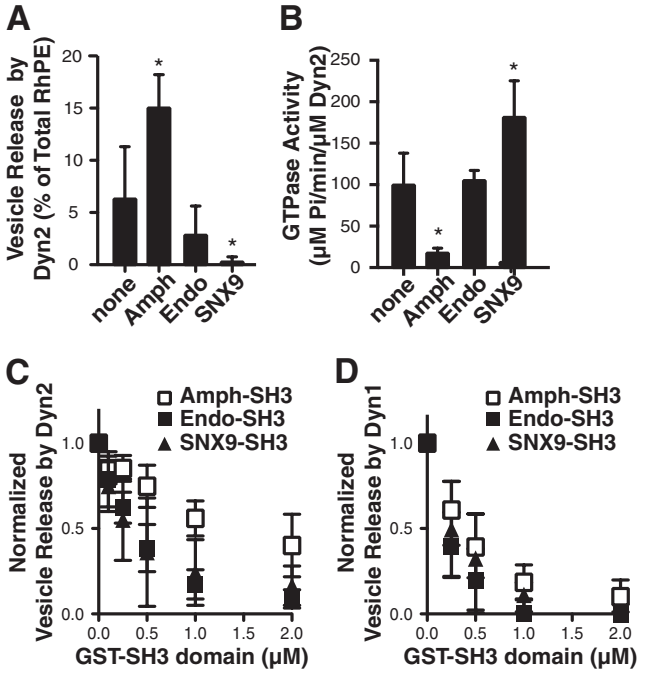

FIGURE 4. **Differential effects of Dyn2 binding partners on vesicle release and assembly-stimulated GTPase activity.** *A*, vesicle release from SUPER templates catalyzed by 0.5 μM full-length Dyn2 assayed alone or in the presence of 0.5 μM amphiphysin, endophilin or SNX9. Fluorescence released in the absence of GTP was subtracted as background (shown are averages ± S.D., $n = 6$, *, $p < 0.005$). *B*, assembly-stimulated GTPase activity of Dyn2 assayed alone or in the presence of the indicated partner measured on 1 μm liposomes (shown are averages ± S.D., $n = 6$, *, $p < 0.01$). *C*, inhibition of vesicle release catalyzed by 2.0 μM Dyn2 in the presence of increasing concentrations of isolated GST-SH3 domains from amphiphysin, endophilin, or SNX9. Fluorescence released in the absence of GTP was subtracted as background (shown are averages ± S.D., $n = 4$). *D*, same as above except incubations contained 0.5 μm Dyn1 and the indicated concentrations of GST-SH3 domains (shown are averages ± S.D., $n = 5$).

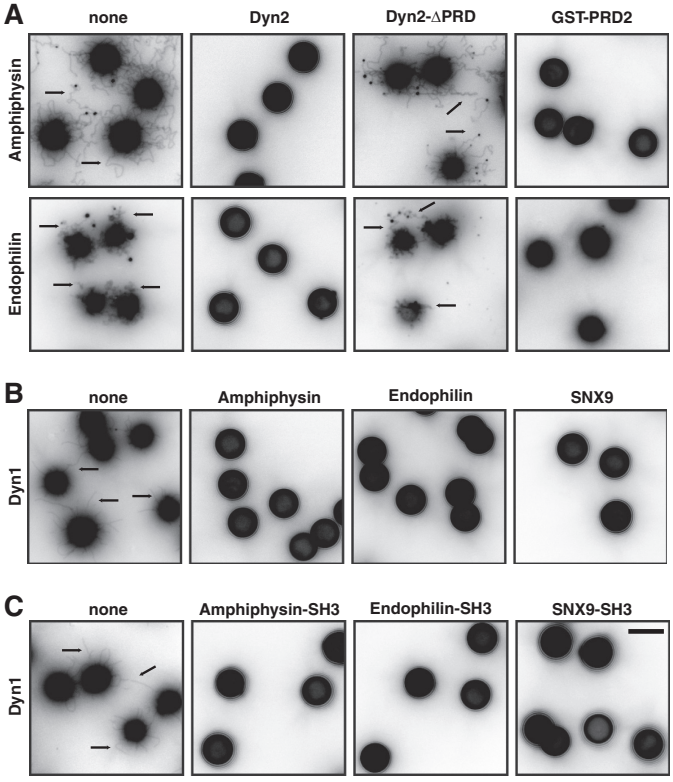

FIGURE 5. **Dynamin and its binding partners limit each others' scaffolding activities.** *A*, tubulation, assayed as described in Fig. 1*A*, by 0.5 μM amphiphysin (*upper panel*) or 0.5 μM endophilin (*lower panel*) in the absence (none) or presence of 0.5 μM Dyn2, Dyn2-ΔPRD or purified GST-PRD of Dyn2 (2.0 μM together with amphiphysin and 0.5 μM together with endophilin). Retraction of amphiphysin coated tubules after addition Dyn2 can be seen in supplemental Movie S2. *B*/*C*, tubulation assays of 0.5 μM Dyn1 in the absence (none) or presence of 0.5 μM amphiphysin, endophilin, or SNX9 (*B*) or their purified GST-tagged SH3 domains (*C*). *Scale bar* is 5 μm. Retraction of Dyn1-coated tubules after addition amphiphysin can be seen in supplemental Movie S3.

rapid collapse (supplemental movie S2). These effects were dependent on PRD-SH3 interactions, as Dyn2-ΔPRD did not inhibit tubulation by amphiphysin or endophilin. Moreover, PRD-SH3 interactions alone were sufficient to inhibit the tubule formation by amphiphysin and endophilin as none were seen when GST-PRD2 was added to the incubation (Fig. 5*A*). Consistent with the weaker inhibitory effect of amph-SH3 on Dyn2-catalyzed vesicle release (Fig. 4*C*), ~4-fold higher concentrations of purified GST-PRD2 were needed to efficiently inhibit tubulation by amphiphysin compared with endophilin (2.0 μM *versus* 0.5 μM, respectively). These differences probably reflect differences in the affinity of PRD2 for amphiphysin-SH3 domain and endophilin-SH3 domain and are likely to account, in part, for the increased ability of full-length Dyn2 to release vesicles in the presence of amphiphysin as compared with endophilin (Fig. 4*A*).

Dyn1, but not Dyn2 will also generate tubules from SUPER templates when incubated in the absence of GTP (Fig. 5*B*). Addition of either amphiphysin, endophilin, or SNX9 (Fig. 5*B*) or their isolated GST-SH3 domains (Fig. 5*C*) prevented the formation of membrane tubules by Dyn1 in these assays. Moreover, addition of amphiphysin caused collapse of preformed Dyn1-coated tubules (supplemental movie S3). Thus, PRD-SH3 interactions reciprocally limit the formation of long scaffolds of dynamin and its N-BAR domain-containing partners.

The ENTH Domain Does Not Facilitate Dyn2-catalyzed Vesicle Release—Epsin encodes an ENTH domain that can also contribute to curvature generation during endocytosis through insertion of its N-terminal amphipathic α-helix (21). When bound to liposomes at sufficiently high concentrations, purified ENTH domains will transform 200 nm diameter liposomes into smaller ~20 nm diameter vesicles and micelles, leading to the suggestion that the ENTH domain alone can mediate membrane fission (32). When incubated with SUPER templates at low concentrations (0.5 μM), unlike N-BAR domains, the ENTH domain fails to generate membrane tubules (Fig. 6*A*). However, at higher concentrations (*e.g.* 10 μM) we observe released vesicles (Fig. 6*A*). Vesicle release by ENTH domains can also be measured by sedimentation and occurs in a concentration-dependent manner above a threshold of ~1 μM, (Fig. 6*B*). We also did not observe a concentration dependent increase in Dyn2-catalyzed vesicle release upon addition of ENTH domain, indicating that, unlike N-BAR domains, the ENTH domain did not function synergistically with Dyn2 (Fig. 6*C*). In contrast to its low ability to release vesicles from planar SUPER templates, Dyn2 can catalyze fission of curved membrane tethers in a manner similar to Dyn1 (9). Therefore, we tested whether fission by the ENTH domain might also be curvature dependent. Upon addition of Dyn2 to tethers drawn

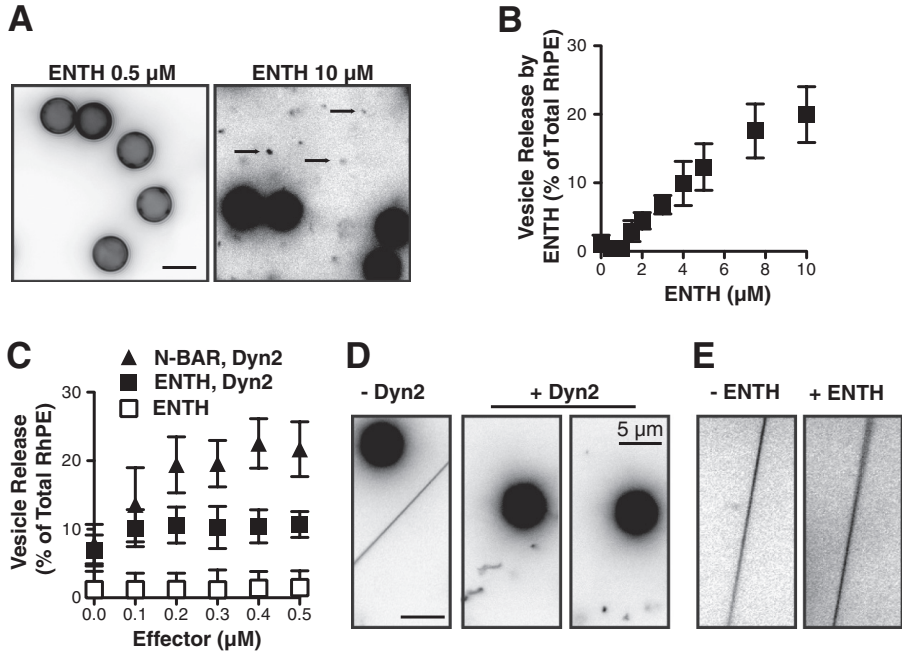

FIGURE 6. **The epsin ENTH domain does not synergistically increase Dyn2-catalyzed vesicle release.** *A*, fluorescent micrographs of SUPER templates in the presence of either 0.5 μM (*left panel*) or 10 μM (*right panel*) purified ENTH domain. SUPER templates were dispersed into assay buffer containing an oxygen scavenger system in the presence of the indicated proteins for 10 min at room temperature. Images are inverted in contrast for clarity, and *arrows* indicate released vesicles. *Scale bar* is 5 μm. *B*, vesicle release mediated by the ENTH domain was measured by the release of fluorescent RhPE into the supernatant after sedimentation of the SUPER templates (shown are averages $\pm$ S.D., $n = 6$). Fluorescence released in the absence of ENTH domain was subtracted as background. *C*, vesicle release from SUPER templates catalyzed by Dyn2 (0.5 μM) in the presence of increasing concentrations of either NBAR domain or by the ENTH domain alone. Fluorescence released in the absence of ENTH domain or GTP for incubations including dynamin was subtracted as background (shown are averages $\pm$ S.D., $n = 6$). *D/E*, fission of membrane tethers. SUPER templates were dispersed into assay buffer containing an oxygen scavenger system and 1 mM GTP. After the templates had settled and membrane tethers were generated, imaging was started, and Dyn2 (***D***) or ENTH (***E***) domains were added to the solution with a pipette to a final concentration of 0.5 μM. The figure shows the field of view before ($t = 0$, *left panel*) and after addition of Dyn2 or ENTH domain. See supplemental Movies S4 and S5 for full sequence and supplemental Movie S6 for the incubation of membrane tethers with 10 μM ENTH domain. *Scale bar* is 5 μm.

from SUPER templates, individual fission events can be seen leaving freely floating Dyn2-coated tubes that can undergo subsequent fission events (Fig. 6*D*, supplemental movie S4). In contrast, fission was only rarely observed in the presence of ENTH domain at the same concentration (Fig. 6*E*, supplemental movie S5). At higher concentrations (*e.g.* 10 μM) fission occurred, but only one breakage of the membrane was observed upon which the uncoated or loosely-coated tether rapidly retracted into the SUPER template (supplemental movie S6). Together these data suggest that while ENTH domains can mediate fission, they do so much less efficiently than either Dyn1 or Dyn2.

DISCUSSION

Our systematic analysis of the BAR domain-containing binding partners of dynamin has revealed a complex set of interactions that regulate the fission, GTPase and scaffolding activities of Dyn2. We have shown that, although their curvature generating N-BAR domains synergize with Dyn2 to catalyze vesicle release, the SH3-PRD interactions are inhibitory. Moreover, these latter interactions reciprocally regulate the scaffolding activities of dynamin and its partners. The three dynamin binding partners we studied, amphiphyisin, endophilin, and SNX9, differentially effect the ability of Dyn2 to catalyze membrane fission, which presumably reflects differences in the relative potency of their positive, curvature generating activities and the negative regulatory effects mediated by SH3 domain interactions. As previously hypothesized (44), these complex patterns of regulation might reflect a cascade of functional interactions that together regulate curvature generation and dynamin activity during CME.

Our findings on the differential regulation of dynamin activity by amphiphysin, endophilin, and SNX9 in part overlap with previous observations and, in part, differ. For example, Farsad *et al.* (45) reported that both amphiphysin and endophilin co-oligomerize with Dyn1 to tubulate liposomes. However, these experiments were performed at protein concentrations ~10-fold higher than those used in our studies. Consistent with our findings, this group also reported differential effects of amphiphysin and endophilin on Dyn1-catalyzed vesiculation (45). A previous study by this group, also reported that amphiphysin enhances dynamin-mediated vesiculation of large liposomes, as measured by dynamic light scattering; however, they showed that amphiphysin stimulated dynamin GTPase activity under these conditions (29). We and others have shown that amphiphysin can inhibit dynamin self-assembly, both in solution (28), and on lipid templates (31). More recently, Meinecke *et al.* (47) reported an interdependence for the recruitment of dynamin and amphiphysin or endophilin to giant unilamellar vesicles (GUVs) that required SH3-PRD interactions. Importantly, these studies focused on recruitment of proteins to the planar surface of GUVs formed under high osmotic stress: there was no evidence of tubulation in this system with either protein alone or in combination. In contrast,

the SUPER templates we use carry a large membrane reservoir and are under low tension (7); hence, they are readily remodeled, even by low concentrations of Dyn1, amphiphysin, or endophilin. Importantly, our studies measure the formation of long, rigid scaffolds that can generate membrane tubules and not membrane adsorption, which is likely to still be occurring under the conditions of our assay. Finally, Meinecke *et al.* (47) also reported that both amphiphysin and endophilin functioned together with Dyn1 to catalyze vesicle release from GUVs. The protein concentrations used in these experiments (1 μM each) were significantly higher than those required for synergistic fission activity with Dyn1. Thus, differences between our results and those reported by others likely reflect differences in the membrane template and protein concentrations used, and in the nature of the assay and activity being measured.

We also did not detect differences in the ability of isolated N-BAR domains *versus* full-length amphiphysin or endophilin to generate tubes from SUPER templates, even at subμM concentrations. Others have suggested that BAR domain-containing proteins are auto-inhibited due to intramolecular interactions (47–52). Consequently, constructs lacking the SH3 domain could bind to and tubulate liposomes or generate membrane tubules more efficiently when overexpressed in cells. This mechanism is best understood for the BAR domain containing dynamin binding partner syndapin (also known as Pacsin) for which auto-inhibition could be released by the interaction of the SH3 domain with the dynamin PRD (50, 53). One possible explanation for these differences is that the N-BAR domains are both curvature generators and curvature sensors. Curved surfaces resulting from fluctuations in the low tension membrane reservoir present on SUPER templates *in vitro* or those generated by other mechanisms *in vivo* might serve as membrane templates capable of activating and recruiting N-BAR domain-containing EAPs (54). Others have suggested that the curvature sensing and generating activities of dynamin and N-BAR domains can create positive feedback loops to enhance membrane tubulation (55).

Two interesting and mechanistically revealing observations from these studies were the reciprocal relationship between the effect of amphiphysin and endophilin on dynamin fission *versus* assembly-stimulated GTPase activities and the reciprocal regulation of each others' scaffolding activities. Shorter scaffolds would lead to overall decreased rates of GTP hydrolysis, which depends on inter-rung interactions (56) and may be critical in facilitating fission activity, because the formation of long scaffolds on membrane tubules/CCP necks will inhibit fission (7, 32, 41). Indeed, recent biophysical measurements and modeling studies of dynamin-catalyzed fission on small lipid nanotubes showed that the optimal fission apparatus consists of a two-rung dynamin collar (40). The authors suggested that one role for GTP hydrolysis and accompanying cycles of assembly/disassembly was to restrict and optimize the size of these short functional units. We hypothesize that N-BAR-mediated curvature generation and SH3-mediated regulation of assembly function coordinately to control the length of protein scaffolds at sites of fission and increase the efficiency of Dyn2-catalyzed vesicle release. That N-BAR domains, even in the absence of direct SH3-mediated interactions with Dyn2 also reciprocally affect fission and GTPase activities, suggest feedback mechanisms between membrane geometry and dynamin activity.

A recent study suggested that bilayer destabilization driven by the insertion of amphipathic helices of the epsin ENTH domain drives membrane fission during CME. In this scenario, the scaffolding activity of dynamin would inhibit fission. GTP hydrolysis, which triggers dynamin disassembly, would serve to temporally regulate epsin-mediated fission (32). This hypothesis was based on the following four observations: 1) Knockdown of epsin impaired CME. 2) Overexpression of epsin, but not endogenously expressed epsin, could rescue transferrin uptake in dynamin knock-out cells. 3) Epsin did not rescue transferrin uptake in cells expressing dominant-negative dynamin mutants defective in GTP hydrolysis, which form stable assemblies 4) Epsin binding and integration into 200 nm liposomes *in vitro* induced the formation of 20 nm vesicles and/or micelles. We tested this hypothesis in our SUPER template system and indeed found that the ENTH domain of epsin could drive vesicle release at high concentrations (10 μM). In contrast, Dyn1 alone or Dyn2 in synergy with N-BAR domains mediated vesicle release at sub-μM concentrations. While Dyn2 alone is less effective at catalyzing vesicle release of planar SUPER templates, it readily catalyzes fission of membrane tethers (9). The liposome fission activity of epsin seen with 200 nm liposomes (32) might also be curvature dependent, as the same group failed to detect fission of larger, 400 nm liposomes of the same lipid composition, even at 40 μM ENTH domain (21). However, we did not observe efficient scission of curved membrane tethers by epsin and similar to SUPER templates, epsin-mediated fission was only observed at high concentrations.

Epsin is a multifunctional protein with multiple protein-interaction motifs. The *Drosophila* homologue of epsin, Liquid facets (Lqf), is essential for endocytosis, but its role is complex as transgenic expression of either the ENTH domain-encoding N terminus or the remaining cargo and coat-interacting C-terminal regions could rescue endocytosis in Lqf-deficient flies (57). Genetic studies in yeast have revealed roles for epsins in recognition of ubiquitinated cargo molecules (58), as a scaffold for assembly and organization of components of the early endocytic machinery (59) and as a platform for actin assembly (60). Studies in mammalian cells have suggested a role for epsin as an adaptor for ubiquitinated cargo (61, 62) and shown that it is recruited early to CCPs along with other adaptor and scaffolding molecules (63), where it potentially regulates early stages of CCP maturation (62). Together, these *in vivo* findings are more consistent with a role for epsin at earlier stages of CME.

In addition to the three proteins studied here, dynamin has numerous other SH3 domain-containing binding partners (*e.g.* cortactin, Abp1, Grb2, and intersectin) implicated in clathrin-mediated endocytosis. The differential effects of amphiphysin, endophilin, and SNX9 on Dyn2-catalyzed fission suggest the possibility that a hierarchy of SH3 domain interactions might regulate Dyn2 function *in vivo*. In this scenario, weak curvature generating SH3 domain-containing proteins (*e.g.* SNX9, intersectin) might function to recruit Dyn2 to CCPs and delay its assembly, thereby acting as early timers for fission. The *in vitro* biochemical properties of amphiphysin suggest that it might

cooperate with Dyn2 during fission. Endophilin, which does not affect Dyn2-catalyzed fission *in vitro* has been suggested to be recruited late to CCPs and to function in recruiting synaptojanin and coordinating uncoating events subsequent to fission (46). Indeed, there is strong evidence for a temporal hierarchy of recruitment of BAR and/or SH3 domain-containing endocytic accessory proteins during CCP maturation (63). However, given the commonality of protein interaction motifs involved and because of the necessity of overexpressing fluorescently tagged proteins, it is likely that higher concentrations of one partner might displace others, thereby disrupting and/or blurring the normal sequence of events. Recent developments in genome-editing and tagging endocytic proteins at their endogenous loci in mammalian cells (37), when coupled to more sensitive methods for detection and tracking (4), should provide clearer insights into these hierarchical relationships.

Acknowledgments—We thank members of the Schmid laboratory and Vadim Frolov (IKERBASQUE, Basque Foundation for Science, Bilbao, Spain) for helpful discussions and for critically reading the manuscript.

REFERENCES

1. Schmid, E. M., and McMahon, H. T. (2007) Integrating molecular and network biology to decode endocytosis. *Nature* **448,** 883–888
2. Rao, Y., Rückert, C., Saenger, W., and Haucke, V. (2012) The early steps of endocytosis: from cargo selection to membrane deformation. *Eur. J. Cell Biol.* **91,** 226–233
3. Mettlen, M., Pucadyil, T., Ramachandran, R., and Schmid, S. L. (2009) Dissecting dynamin's role in clathrin-mediated endocytosis. *Biochem. Soc. Trans.* **37,** 1022–1026
4. Aguet, F., Antonescu, C. N., Mettlen, M., Schmid, S. L., and Danuser, G. (2013) Advances in Analysis of Low Signal-to-Noise Images Link Dynamin and AP2 to the Functions of an Endocytic Checkpoint. *Dev. Cell*, 10.1016/j.devcel.2013.06.019
5. Schmid, S. L., and Frolov, V. A. (2011) Dynamin: functional design of a membrane fission catalyst. *Annu. Rev. Cell Dev. Biol.* **27,** 79–105
6. Ferguson, S. M., and De Camilli, P. (2012) Dynamin, a membrane-remodelling GTPase. *Nat. Rev. Mol. Cell Biol.* **13,** 75–88
7. Pucadyil, T. J., and Schmid, S. L. (2008) Real-Time Visualization of Dynamin-Catalyzed Membrane Fission and Vesicle Release. *Cell* **135,** 1263–1275
8. Pucadyil, T. J., and Schmid, S. L. (2010) Supported bilayers with excess membrane reservoir: a template for reconstituting membrane budding and fission. *Biophys. J.* **99,** 517–525
9. Liu, Y.-W., Neumann, S., Ramachandran, R., Ferguson, S. M., Pucadyil, T. J., and Schmid, S. L. (2011) Differential curvature sensing and generating activities of dynamin isoforms provide opportunities for tissue-specific regulation. *Proc. Natl. Acad. Sci.* **108,** E234—E242
10. Lee, E., Marcucci, M., Daniell, L., Pypaert, M., Weisz, O. A., Ochoa, G.-C., Farsad, K., Wenk, M. R., and De Camilli, P. (2002) Amphiphysin 2 (Bin1) and T-tubule biogenesis in muscle. *Science* **297,** 1193–1196
11. Kamioka, Y., Fukuhara, S., Sawa, H., Nagashima, K., Masuda, M., Matsuda, M., and Mochizuki, N. (2004) A novel dynamin-associating molecule, formin-binding protein 17, induces tubular membrane invaginations and participates in endocytosis. *J. Biol. Chem.* **279,** 40091–40099
12. Peter, B. J., Kent, H. M., Mills, I. G., Vallis, Y., Butler, P. J. G., Evans, P. R., and McMahon, H. T. (2004) BAR domains as sensors of membrane curvature: the amphiphysin BAR structure. *Science* **303,** 495–499
13. Itoh, T., Erdmann, K. S., Roux, A., Habermann, B., Werner, H., and De Camilli, P. (2005) Dynamin and the actin cytoskeleton cooperatively regulate plasma membrane invagination by BAR and F-BAR proteins. *Dev. Cell* **9,** 791–804
14. Masuda, M., Takeda, S., Sone, M., Ohki, T., Mori, H., Kamioka, Y., and Mochizuki, N. (2006) Endophilin BAR domain drives membrane curvature by two newly identified structure-based mechanisms. *EMBO J.* **25,** 2889–2897
15. Shin, N., Ahn, N., Chang-Ileto, B., Park, J., Takei, K., Ahn, S.-G., Kim, S.-A., Di Paolo, G., and Chang, S. (2008) SNX9 regulates tubular invagination of the plasma membrane through interaction with actin cytoskeleton and dynamin 2. *J. Cell Sci.* **121,** 1252–1263
16. Tarricone, C., Xiao, B., Justin, N., Walker, P. A., Rittinger, K., Gamblin, S. J., and Smerdon, S. J. (2001) The structural basis of Arfaptin-mediated cross-talk between Rac and Arf signalling pathways. *Nature* **411,** 215–219
17. Weissenhorn, W. (2005) Crystal structure of the endophilin-A1 BAR domain. *J. Mol. Biol.* **351,** 653–661
18. Gallop, J. L., Jao, C. C., Kent, H. M., Butler, P. J. G., Evans, P. R., Langen, R., and McMahon, H. T. (2006) Mechanism of endophilin N-BAR domain-mediated membrane curvature. *EMBO J.* **25,** 2898–2910
19. Bhatia, V. K., Madsen, K. L., Bolinger, P.-Y., Kunding, A., Hedegård, P., Gether, U., and Stamou, D. (2009) Amphipathic motifs in BAR domains are essential for membrane curvature sensing. *EMBO J.* **28,** 3303–3314
20. Jao, C. C., Hegde, B. G., Gallop, J. L., Hegde, P. B., McMahon, H. T., Haworth, I. S., and Langen, R. (2010) Roles of amphipathic helices and the bin/amphiphysin/rvs (BAR) domain of endophilin in membrane curvature generation. *J. Biol. Chem.* **285,** 20164–20170
21. Ford, M. G. J., Mills, I. G., Peter, B. J., Vallis, Y., Praefcke, G. J. K., Evans, P. R., and McMahon, H. T. (2002) Curvature of clathrin-coated pits driven by epsin. *Nature* **419,** 361–366
22. Stahelin, R. V., Long, F., Peter, B. J., Murray, D., De Camilli, P., McMahon, H. T., and Cho, W. (2003) Contrasting membrane interaction mechanisms of AP180 N-terminal homology (ANTH) and epsin N-terminal homology (ENTH) domains. *J. Biol. Chem.* **278,** 28993–28999
23. Yoon, Y., Tong, J., Lee, P. J., Albanese, A., Bhardwaj, N., Källberg, M., Digman, M. A., Lu, H., Gratton, E., Shin, Y.-K., and Cho, W. (2010) Molecular basis of the potent membrane-remodeling activity of the epsin 1 N-terminal homology domain. *J. Biol. Chem.* **285,** 531–540
24. Lai, C.-L., Jao, C. C., Lyman, E., Gallop, J. L., Peter, B. J., McMahon, H. T., Langen, R., and Voth, G. A. (2012) Membrane binding and self-association of the epsin N-terminal homology domain. *J. Mol. Biol.* **423,** 800–817
25. Gout, I., Dhand, R., Hiles, I. D., Fry, M. J., Panayotou, G., Das, P., Truong, O., Totty, N. F., Hsuan, J., and Booker, G. W. (1993) The GTPase dynamin binds to and is activated by a subset of SH3 domains. *Cell* **75,** 25–36
26. Herskovits, J. S., Shpetner, H. S., Burgess, C. C., and Vallee, R. B. (1993) Microtubules and Src homology 3 domains stimulate the dynamin GTPase via its C-terminal domain. *Proc. Natl. Acad. Sci. U.S.A.* **90,** 11468–11472
27. Wigge, P., Köhler, K., Vallis, Y., Doyle, C. A., Owen, D., Hunt, S. P., and McMahon, H. T. (1997) Amphiphysin heterodimers: potential role in clathrin-mediated endocytosis. *Mol. Biol. Cell* **8,** 2003–2015
28. Owen, D. J., Wigge, P., Vallis, Y., Moore, J. D., Evans, P. R., and McMahon, H. T. (1998) Crystal structure of the amphiphysin-2 SH3 domain and its role in the prevention of dynamin ring formation. *EMBO J.* **17,** 5273–5285
29. Yoshida, Y., Kinuta, M., Abe, T., Liang, S., Araki, K., Cremona, O., Di Paolo, G., Moriyama, Y., Yasuda, T., De Camilli, P., and Takei, K. (2004) The stimulatory action of amphiphysin on dynamin function is dependent on lipid bilayer curvature. *EMBO J.* **23,** 3483–3491
30. Soulet, F., Yarar, D., Leonard, M., and Schmid, S. L. (2005) SNX9 regulates dynamin assembly and is required for efficient clathrin-mediated endocytosis. *Mol. Biol. Cell* **16,** 2058–2067
31. Ramachandran, R., and Schmid, S. L. (2008) Real-time detection reveals that effectors couple dynamin's GTP-dependent conformational changes to the membrane. *EMBO J.* **27,** 27–37
32. Boucrot, E., Pick, A., Çamdere, G., Liska, N., Evergren, E., McMahon, H. T., and Kozlov, M. M. (2012) Membrane fission is promoted by insertion of amphipathic helices and is restricted by crescent BAR domains. *Cell* **149,** 124–136
33. Ramachandran, R., Pucadyil, T. J., Liu, Y.-W., Acharya, S., Leonard, M., Lukiyanchuk, V., and Schmid, S. L. (2009) Membrane insertion of the pleckstrin homology domain variable loop 1 is critical for dynamin-catalyzed vesicle scission. *Mol. Biol. Cell* **20,** 4630–4639

34. Stowell, M. H., Marks, B., Wigge, P., and McMahon, H. T. (1999) Nucleotide-dependent conformational changes in dynamin: evidence for a mechanochemical molecular spring. *Nat. Cell Biol.* **1,** 27–32
35. Neumann, S., Pucadyil, T. J., and Schmid, S. L. (2013) Analyzing membrane remodeling and fission using supported bilayers with excess membrane reservoir. *Nat. Protoc.* **8,** 213–222
36. Leonard, M., Song, B. D., Ramachandran, R., and Schmid, S. L. (2005) Robust colorimetric assays for dynamin's basal and stimulated GTPase activities. *Methods Enzymol.* **404,** 490–503
37. Doyon, J. B., Zeitler, B., Cheng, J., Cheng, A. T., Cherone, J. M., Santiago, Y., Lee, A. H., Vo, T. D., Doyon, Y., Miller, J. C., Paschon, D. E., Zhang, L., Rebar, E. J., Gregory, P. D., Urnov, F. D., and Drubin, D. G. (2011) Rapid and efficient clathrin-mediated endocytosis revealed in genome-edited mammalian cells. *Nat. Cell Biol.* **13,** 331–337
38. Ramachandran, R., Surka, M., Chappie, J. S., Fowler, D. M., Foss, T. R., Song, B. D., and Schmid, S. L. (2007) The dynamin middle domain is critical for tetramerization and higher-order self-assembly. *EMBO J.* **26,** 559–566
39. Liu, Y.-W., Mattila, J.-P., and Schmid, S. L. (2013) Dynamin-catalyzed membrane fission requires coordinated GTP hydrolysis. *PLoS ONE* **8,** e55691
40. Shnyrova, A. V., Bashkirov, P. V., Akimov, S. A., Pucadyil, T. J., Zimmerberg, J., Schmid, S. L., and Frolov, V. A. (2013) Geometric catalysis of membrane fission driven by flexible dynamin rings. *Science* **339,** 1433–1436
41. Bashkirov, P. V., Akimov, S. A., Evseev, A. I., Schmid, S. L., Zimmerberg, J., and Frolov, V. A. (2008) GTPase cycle of dynamin is coupled to membrane squeeze and release, leading to spontaneous fission. *Cell* **135,** 1276–1286
42. Pylypenko, O., Lundmark, R., Rasmuson, E., Carlsson, S. R., and Rak, A. (2007) The PX-BAR membrane-remodeling unit of sorting nexin 9. *EMBO J.* **26,** 4788–4800
43. Yarar, D., Surka, M. C., Leonard, M. C., and Schmid, S. L. (2008) SNX9 activities are regulated by multiple phosphoinositides through both PX and BAR domains. *Traffic* **9,** 133–146
44. Qualmann, B., Koch, D., and Kessels, M. M. (2011) Let's go bananas: revisiting the endocytic BAR code. *EMBO J.* **30,** 3501–3515
45. Farsad, K., Ringstad, N., Takei, K., Floyd, S. R., Rose, K., and De Camilli, P. (2001) Generation of high curvature membranes mediated by direct endophilin bilayer interactions. *J. Cell Biol.* **155,** 193–200
46. Gad, H., Ringstad, N., Löw, P., Kjaerulff, O., Gustafsson, J., Wenk, M., Di Paolo, G., Nemoto, Y., Crun, J., Ellisman, M. H., De Camilli, P., Shupliakov, O., and Brodin, L. (2000) Fission and uncoating of synaptic clathrin-coated vesicles are perturbed by disruption of interactions with the SH3 domain of endophilin. *Neuron* **27,** 301–312
47. Meinecke, M., Boucrot, E., Camdere, G., Hon, W.-C., Mittal, R., and McMahon, H. T. (2013) Cooperative recruitment of Dynamin and BAR domain-containing proteins leads to GTP-dependent membrane scission. *J. Biol. Chem.* **288,** 6651–6661
48. Kojima, C., Hashimoto, A., Yabuta, I., Hirose, M., Hashimoto, S., Kanaho, Y., Sumimoto, H., Ikegami, T., and Sabe, H. (2004) Regulation of Bin1 SH3 domain binding by phosphoinositides. *EMBO J.* **23,** 4413–4422
49. Wang, Q., Kaan, H. Y., Hooda, R. N., Goh, S. L., and Sondermann, H. (2008) Structure and plasticity of Endophilin and Sorting Nexin 9. *Structure* **16,** 1574–1587
50. Wang, Q., Navarro, M. V., Peng, G., Molinelli, E., Goh, S. L., Judson, B. L., Rajashankar, K. R., and Sondermann, H. (2009) Molecular mechanism of membrane constriction and tubulation mediated by the F-BAR protein Pacsin/Syndapin. *Proc. Natl. Acad. Sci.* **106,** 12700–12705
51. Rao, Y., Ma, Q., Vahedi-Faridi, A., Sundborger, A., Pechstein, A., Puchkov, D., Luo, L., Shupliakov, O., Saenger, W., and Haucke, V. (2010) Molecular basis for SH3 domain regulation of F-BAR-mediated membrane deformation. *Proc. Natl. Acad. Sci.* **107,** 8213–8218
52. Vázquez, F. X., Unger, V. M., and Voth, G. A. (2013) Autoinhibition of Endophilin in Solution via Interdomain Interactions. *Biophys. J.* **104,** 396–403
53. Goh, S. L., Wang, Q., Byrnes, L. J., and Sondermann, H. (2012) Versatile membrane deformation potential of activated pacsin. *PLoS ONE* **7,** e51628
54. Liu, J., Sun, Y., Oster, G. F., and Drubin, D. G. (2010) Mechanochemical crosstalk during endocytic vesicle formation. *Curr. Opin. Cell Biol.* **22,** 36–43
55. Roux, A., Koster, G., Lenz, M., Sorre, B., Manneville, J.-B., Nassoy, P., and Bassereau, P. (2010) Membrane curvature controls dynamin polymerization. *Proc. Natl. Acad. Sci.* **107,** 4141–4146
56. Chappie, J. S., Mears, J. A., Fang, S., Leonard, M., Schmid, S. L., Milligan, R. A., Hinshaw, J. E., and Dyda, F. (2011) A pseudoatomic model of the dynamin polymer identifies a hydrolysis-dependent powerstroke. *Cell* **147,** 209–222
57. Overstreet, E., Chen, X., Wendland, B., and Fischer, J. A. (2003) Either part of a *Drosophila* epsin protein, divided after the ENTH domain, functions in endocytosis of delta in the developing eye. *Curr. Biol.* **13,** 854–860
58. Shih, S. C., Katzmann, D. J., Schnell, J. D., Sutanto, M., Emr, S. D., and Hicke, L. (2002) Epsins and Vps27p/Hrs contain ubiquitin-binding domains that function in receptor endocytosis. *Nat. Cell Biol.* **4,** 389–393
59. Dores, M. R., Schnell, J. D., Maldonado-Baez, L., Wendland, B., and Hicke, L. (2010) The function of yeast epsin and Ede1 ubiquitin-binding domains during receptor internalization. *Traffic* **11,** 151–160
60. Skruzny, M., Brach, T., Ciuffa, R., Rybina, S., Wachsmuth, M., and Kaksonen, M. (2012) Molecular basis for coupling the plasma membrane to the actin cytoskeleton during clathrin-mediated endocytosis. *Proc. Natl. Acad. Sci.* **109,** E2533–E2542
61. Kazazic, M., Bertelsen, V., Pedersen, K. W., Vuong, T. T., Grandal, M. V., Rødland, M. S., Traub, L. M., Stang, E., and Madshus, I. H. (2009) Epsin 1 is involved in recruitment of ubiquitinated EGF receptors into clathrin-coated pits. *Traffic* **10,** 235–245
62. Henry, A. G., Hislop, J. N., Grove, J., Thorn, K., Marsh, M., and von Zastrow, M. (2012) Regulation of endocytic clathrin dynamics by cargo ubiquitination. *Dev. Cell* **23,** 519–532
63. Taylor, M. J., Perrais, D., and Merrifield, C. J. (2011) A high precision survey of the molecular dynamics of mammalian clathrin-mediated endocytosis. *PLoS Biol.* **9,** e1000604